International Journal of GEOMATE, Jan., 2024 Vol.26, Issue 113, pp.66-73
ISSN: 2186-2982 (P), 2186-2990 (O), Japan, DOI: https://doi.org/10.21660/2024.113.g13202
Geotechnique, Construction Materials and Environment

DEVELOPMENT OF CONTACT AREA MODEL FOR MOTORCYCLE TIRE HYDROPLANING THROUGH EXPERIMENTAL INVESTIGATION

Weerachai Chaiworapuek [1], Chakrit Suvanjumrat[2], Natnaree Worajinda[2] and Ravivat Rugsaj [3*]

[1]Department of Mechanical Engineering, Faculty of Engineering, Kasetsart University, Thailand;
[2]Department of Mechanical Engineering, Faculty of Engineering, Mahidol University, Thailand;
[3]Department of Mechatronics Engineering and Artificial Intelligence, Vincent Mary School of Engineering, Assumption University, Thailand

*Corresponding Author, Received: 15 June 2023, Revised: 16 Dec. 2023, Accepted: 18 Dec. 2023

ABSTRACT: Hydroplaning, a phenomenon prevalent in high-speed vehicle movement on wet surfaces, poses a significant risk by compromising tire traction and inducing slippage. This risk is particularly pronounced in motorcycles due to their reduced surface area and heightened susceptibility to rollovers. The hydroplaning force acting on motorcycle tires is intricately tied to tire-ground interaction and tire contact characteristics. This study endeavors to formulate a mathematical model to predict the contact area and contact pressure of motorcycle tires, with a specific focus on the impact of tread and groove geometries. A set of 2.5-17 inch motorcycle tires commonly used in Thailand was selected for comprehensive investigation. Eight commercially available tires, each featuring distinct tread and groove profiles, underwent testing utilizing a vertical tire testing machine. Standardized conditions, encompassing a vertical load of 850 N and an inflation pressure of 29 psi, were consistently applied. Testing was conducted at five positions along the tire circumference to minimize position-related variability, and results were averaged for accuracy. Pressure measurement film captured footprints at each load and inflation pressure, with a conversion algorithm employed for interpretation. The resultant mathematical model seeks to elucidate the dynamic alterations in the tire-ground contact area and predict both the contact area and contact pressure. This model's applicability extends to forecasting hydroplaning forces for motorcycle tires with diverse tread and groove profiles, thereby contributing valuable insights to the broader understanding of tire characteristics and enhancing safety considerations for motorcycles.

Keywords: Experiment, Hydroplaning, Footprint, Motorcycle, Tire

1. INTRODUCTION

The tire-ground contact area and contact pressure stand out as crucial parameters influencing various aspects of tire performance and characteristics. These factors play a pivotal role in determining a tire's traction, the wear of its tread, and its capability to resist hydroplaning. Hydroplaning, a hydrodynamic occurrence observed when tires roll on wet roads at high speeds, poses a significant safety concern as it can lead to a loss of vehicle control. Several elements contribute to hydroplaning, including the vehicle's speed, the depth of water on the road, and the tire's ability to effectively disperse water. Notably, the tire's sculpture, architecture, and pressure impact hydroplaning, even if the grooves or void volume of the tread are identical. Thus, the design of tire tread patterns must carefully consider hydroplaning to ensure optimal dynamic performance and, ultimately, driver safety [1].

Estimating hydroplaning force involves employing a mathematical model typically derived from the Bernoulli equation. The groundwork for understanding hydroplaning buoyancy force and proposing the equation was laid by Horne et al. [2-4]. Empirical equations, developed through experimental efforts, have been crucial in predicting hydroplaning speeds on various tire and road types. The widely accepted prediction model is a combined one, integrating Gallaway's equation [5, 6] and Huebner's equation [7]. Analogous to lift force acting on an airfoil against airflow, tire hydroplaning is conceptualized as generating lift forces. These lift forces, contingent on different water depths, are estimated using Bernoulli's equation [8, 9]. Notably, the tire's contact parameters, including contact area, play a pivotal role in determining the hydroplaning force within these equations.

Estimating a tire's contact parameters involves a combination of experimental methods and finite element analysis (FEA) [10-12]. In the context of hydroplaning performance evaluation, the loss of the tire's contact force serves as a key indicator. For truck tires, the required contact pressure was estimated based on collected data, and a fluid flow model was validated using finite element methods

(FEM), finite difference methods (FDM), and asymptotic methods [13, 14]. Investigation into the cornering performance of truck tires on wet surfaces included obtaining adhesion coefficients through experiments, comparing them to FEA and smoothed particle hydrodynamics (SPH) analysis [15, 16]. The mechanical behavior of solid tires was modeled using a hyperelastic constitutive model, and numerical analysis of tire deformation tests was conducted through FEA [17, 18]. The contact patch of solid tires, measured using a tire testing machine and pressure measurement film, showed good agreement with FEA models [19]. Further analysis involved developing FEA models for contact patch analysis against flat and curved surfaces, comparing solid tire behavior on tire testing and drum testing machines, and proposing appropriate ratios for accurate simulation results on curved surfaces [20, 21]. Additionally, an airless tire with a novel spoke structure designed for skid steer loaders underwent FEA for analyzing contact interaction with the ground [22-25], while its mechanical characteristics were investigated through laboratory testing [26].

Despite the utility of numerical analysis and experiments in estimating tire contact characteristics, there remains a need for studies focusing on contact parameters under various tire operating conditions. The objective of this research is to create a mathematical model for the contact area of motorcycle tires, considering different tread and groove profiles. Notably, the approach involves using an equation derived from a smooth tread motorcycle tire, aiming to eliminate dependencies on specific tread patterns. This strategy enhances the generalizability of the model, allowing for a more comprehensive understanding of tire contact characteristics across diverse operating conditions.

2. RESEARCH SIGNIFICANCE

Hydroplaning occurs when vehicles travel at high speeds on a wet surface with sufficient water depth. It causes the tires to lose traction, leading to potential slippage. This is particularly true for motorcycle tires due to their smaller surface area, making them more susceptible to rolling over compared to other vehicles. Additionally, motorcycle riders face a higher risk of injury or fatality in accidents. The hydroplaning force is heavily influenced by the interaction between the tires and the road, taking into account factors such as contact area and contact pressure. Therefore, it is essential to develop a mathematical model for the contact area of motorcycle tires, considering various tread and groove profiles.

3. MATERIALS AND METHODS

3.1 Vertical Stiffness and Footprint Tests of Smooth-Tread Motorcycle Tire

In the initial phase of the study, the focus was on analyzing the contact area, contact pressure, footprint, and vertical stiffness of a smooth tread or slick motorcycle tire. This was carried out using a specialized tire testing machine, the Ektron PL-2003, developed by Ektron Tek Co., Ltd. To eliminate the influence of tread patterns, experiments were conducted on a tire mounted on the testing axle, with its rotation fixed by means of an adapter. Additionally, footprint and contact pressure were measured using a Fuji Prescale LLLW PS 270x220 5S-E pressure measurement film. The experimentation involved varying the inflation pressure within the range of 29, 31, 33, and 35 psi (200, 213.74, 227.53, 241.32 kPa) to investigate the impact on contact area and footprint. Simultaneously, the load was adjusted to 550, 650, 750, and 850 N, with the maximum load set at 850 N to align with the combined allowable weight of the motorcycle, driver, and passenger.

During the experiments, the testing plate ascended to exert pressure on the tire until the targeted load was achieved. The pressing force and vertical displacement were meticulously recorded through a load cell and position transducer,

Fig.1 Mounting of a smooth tread motorcycle tire on the tire testing machine

respectively. To ensure robustness in the findings, tests were conducted at three angular positions for each loading condition, mitigating any randomness associated with the tire's circumference position. Following the full application of load, the

motorcycle tire was systematically rotated to new angular positions. The mounting process of a smooth tread motorcycle tire on the tire testing machine and the installation of the pressure measurement film are illustrated in Figures 1 and 2, respectively.

Fig.2 Pressure measurement film.

4. RESULTS AND DISCUSSION

4.1 Modeling of Footprint Area for Smooth-Tread Motorcycle Tire

The tire testing machine was employed to gather data on the vertical force, displacement at the tire center, and various contact parameters of a smooth-tread motorcycle tire. These parameters encompassed the tire's gross area, contact area, average contact pressure, area fraction, and maximum contact pressure. Additionally, the vertical stiffness was estimated from the ratio between vertical force and displacement. Using a conversion algorithm based on pressure, contact pressure distribution and maximum contact pressure were estimated. The collected contact parameters for the smooth tread tire under different inflation pressures and loads are summarized as shown in Table 1. Visual representations of the total contact area and maximum contact pressure under different loads and pressures are depicted in Figures 3 and 4, respectively.

It was observed that the contact area exhibited a linear increase with higher vertical loads, and similarly, it tended to rise with inflation pressure, especially in the higher load range. This effect was less pronounced at lower load ranges. Conversely,

Table 1 Contact parameters of smooth tread motorcycle tire at different inflation pressures and load

Inflation Pressure (psi)	Load (N)	Vertical stiffness (N/mm)	Gross area (cm^2)	Contact area (cm^2)	Average contact pressure (Pa)	Fraction (%)	Maximum contact pressure (Pa)
29 (200 kPa)	550	69.00	19.14	13.11	0.42	68.48	6.17
	650	69.12	21.53	14.67	0.44	68.12	7.05
	750	73.64	25.07	17.13	0.44	68.32	8.01
	850	92.70	29.2	19.36	0.44	66.3	17.19
31 (213.74 kPa)	550	90.34	15.73	10.86	0.51	69.02	4.79
	650	82.72	22.83	17.42	0.37	76.33	5.07
	750	74.98	23.27	17.52	0.43	75.3	5.98
	850	80.73	28.13	21.46	0.40	76.28	10.02
33 (227.53 kPa)	550	82.93	14.68	10.26	0.54	69.94	6.51
	650	82.06	18.73	13.82	0.47	73.81	7.13
	750	79.34	22.62	16.99	0.44	75.1	7.75
	850	85.79	26.67	20.38	0.42	76.39	15.48
35 (241.32 kPa)	550	97.83	16.89	12.05	0.46	71.35	6.62
	650	97.79	18.69	13.93	0.47	74.52	7.59
	750	88.67	25.7	19.94	0.38	77.6	7.45
	850	95.18	28.83	22.65	0.38	78.56	15.98

the maximum contact pressure displayed a slight linear increase at lower loads but showed a more substantial increase at higher loads. These phenomena can be elucidated by considering the mechanics of the tire contacting area. At lower load ranges, the tire treads were not fully in contact with the testing surface or pavement. As the load increased, the treads gradually made contact, resulting in an increased contact area. Continued load increase led to a point of equilibrium where the applied force became focused on critical tread areas.

The mathematical model expressing the relationship between the contact area of a smooth-tread motorcycle tire, the vertical load, and the inflation pressure can be formulated using a linear regression technique. In this model, the contact area (A_s) is a function of the vertical load (F) and inflation pressure (P), and can be represented as:

$$A_s(P,\mathrm{F}) = (0.0025715P - 0.051776)F - 1.711425P + 49.33725 \quad (1)$$

or,

$$A_s(P,\mathrm{F}) = 0.0025715PF - 0.051776F - 1.711425P + 49.33725 \quad (2)$$

where A_s denotes contact area of a smooth tread motorcycle, P denotes inflation pressure, and F denotes vertical load. The error of the developed equation was estimated to be 5.72% while the coefficient of determination (R^2) was found to be 0.91048.

4.2 Footprint Test for Motorcycle Tires with Different Treads and Groove Profiles

In this segment, we delved into the examination of contact parameters associated with motorcycle tires featuring diverse tread and groove profiles. The focus of our research centered on motorcycle tires sized 2.5-17 inches, a dimension widely utilized and well-suited for motorcycles in Thailand. We meticulously selected eight motorcycle tires, commercially available and popular in the Thai market, to undergo comprehensive testing. Among these, the smoothed tread or slick motorcycle tire, previously examined in the preceding section, served as a reference for its anticipated maximum values in the contact area and other contact parameters. The varied tread and groove profiles of the chosen motorcycle tires are visually depicted in Figure 6, where they are labeled as type A, type B, type C, type D, type E, type F, type G, and type H, respectively.

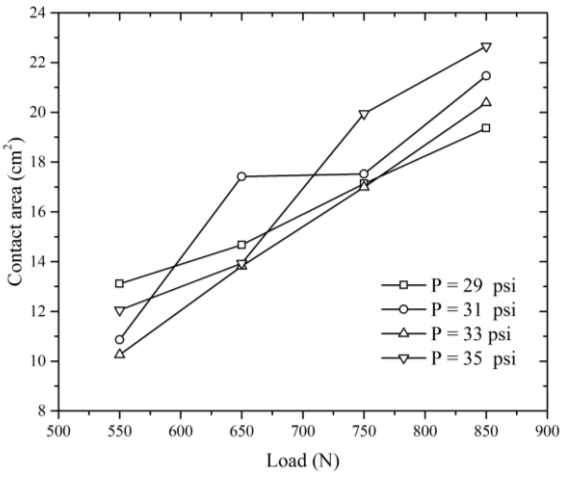

Fig.3 Contact area of smooth tread motorcycle tire at various load and inflation pressure

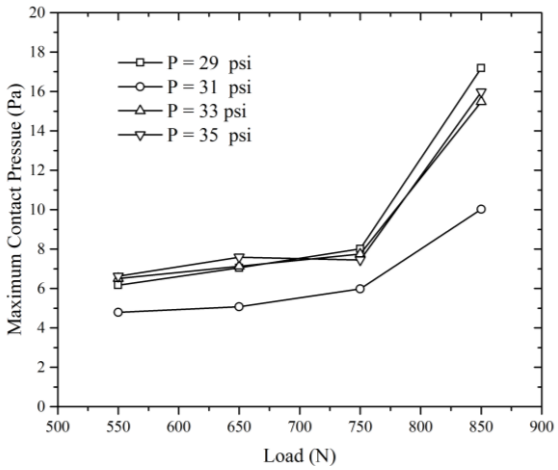

Fig.4 Contact pressure of smooth tread motorcycle tire at various load and inflation pressure

The tire testing machine, along with pressure measurement films, was employed to gather data on the gross area, contact area, groove area, contact pressure, and footprint of motorcycle tires featuring diverse tread and groove profiles, mirroring the methodology employed in the preceding section. A standardized vertical load of 850 N and an inflation pressure of 29 psi were uniformly applied to all motorcycle tires, ensuring consistency across different groove profiles. The resultant footprints of motorcycle tires, each characterized by unique tread and groove patterns, are visually represented in Figure 6. To estimate the groove area for each tire, we approximated it by subtracting the contact area from the overall gross area. Consequently, the groove volume was derived by multiplying the estimated groove area with the groove depth.

Fig.5 Motorcycle tires with different treads and groove profiles.

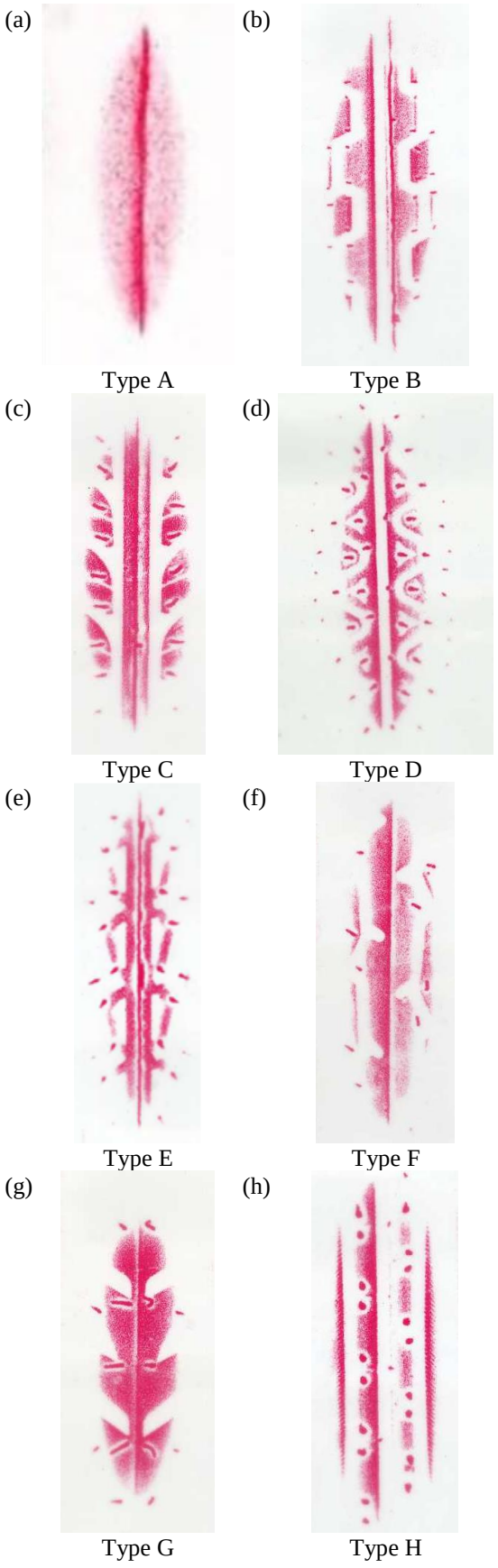

Fig.6 Footprint of motorcycle tires with different tread and groove profiles.

Table 2 Contact parameters of motorcycle tires with various tread and groove profiles at different inflation pressures and loads

Groove type	Gross Area (cm^2)	Contact Area (cm^2)	Groove Area (cm^2)	Groove Depth (cm)	Groove Volume (cm^3)
Type A	29.2	19.36	0	0	0
Type B	36.49	17.05	19.44	0.37	7.1928
Type C	19.07	11.08	7.99	0.41	3.2759
Type D	27.58	12.71	14.87	0.2745	4.081815
Type E	21.64	11.93	9.71	0.275	2.67025
Type G	29.39	16.71	12.68	0.41	5.1988
Type H	21.83	15.23	6.6	0.36	2.376
Type H	36.69	13.47	23.22	0.34	7.8948

The comprehensive set of tire contact parameters, encompassing contact area, groove area, groove depth, and groove volume for motorcycle tires with distinct tread and groove profiles, is succinctly presented in Table 2.

The mathematical model for the contact area, incorporating a groove factor as a function of vertical load and inflation pressure, can be obtained by adapting equation (2) with the addition of this new factor. Subsequently, a linear regression technique was employed to estimate the groove factor function by integrating the contact values gathered from both Table 1 and Table 2. The resulting coefficient of the groove factor can be expressed in the form of a linear equation, as follows:

$$C_g = 1 - 0.038035 A_g \tag{3}$$

where C_g denotes the groove factor coefficient as a function of the groove area, and A_g denotes the groove area for motorcycle tires sized 2.5-17 inches with different tread and groove profiles. Therefore, the empirical mathematical model for predicting the hydroplaning force exerted on motorcycle tires with sizes ranging from 2.5 to 17 inches can be derived by incorporating the groove factor function, C_g, into Equation (2). The resulting expression is as follows:

$$A(P,\mathrm{F}) = C_g A_s \tag{4}$$

or,

$$A(P,\mathrm{F}) = \left(1 - 0.038035 A_g\right) \times \begin{pmatrix} \left(0.0025715P - 0.051776\right)F \\ -1.711425P + 49.33725 \end{pmatrix} \tag{5}$$

The developed equation exhibited an estimated error of 26.48%, with a coefficient of determination (R^2) calculated to be 0.88178. The observed error was attributed to significant disparities in the alignment and orientation of tread and groove profiles. Despite this, the developed equation demonstrated acceptable accuracy. Consequently, the model can effectively predict the tire-ground contact area for motorcycle tires featuring diverse tread and groove profiles across varying loads and inflation pressures, with only the groove area as a required parameter. This outcome positions the model as a valuable tool for predicting tire characteristics. Moreover, it can be instrumental in advancing the development of additional tire characteristic models, such as a mathematical representation of hydroplaning forces for motorcycle tires with distinct tread and groove profiles.

5. CONCLUSION

In this study, a comprehensive mathematical model for the contact area of motorcycle tires was established, exploring the impacts of varying inflation pressure and vertical load on footprint, contact area, and contact pressure.

A vertical stiffness test was conducted on a smooth-tread motorcycle using a tire testing machine. The findings indicated a linear increase in contact area with rising vertical load and inflation pressure, with this effect being more pronounced at higher loads. Conversely, at lower load ranges, the relationship was less evident. Meanwhile, the maximum contact pressure exhibited a slight linear increase at lower loads but demonstrated a considerable rise at higher loads. The mathematical

model for tire-ground contact area, as a function of vertical load and inflation pressure for smooth-tread motorcycle tires, was formulated using a linear regression technique. The developed equation demonstrated a 5.72% error and a coefficient of determination (R^2) of 0.91048, attesting to its accuracy. Subsequently, the model was extended to encompass motorcycle tires with various tread and groove profiles by introducing a groove factor. Despite an estimated error of 26.48%, the R^2 of 0.88178 confirms the utility of the proposed mathematical model for contact area. This robust model offers accuracy and holds promise for further advancements in tire characteristic modeling, including the development of a mathematical model for hydroplaning forces on motorcycle tires with diverse tread and groove profiles.

6. ACKNOWLEDGMENTS

This research received crucial financial support from the Rubber Technology Research Center (RTEC) at Mahidol University, as well as the Thailand Research Fund (TRF) through the TRF Research Grant No. RDG62T0026. Additionally, the Faculty of Engineering at Kasetsart University played a pivotal role by providing support through Research Grant No. Post Doc.65/02/ME. These funding sources were instrumental in facilitating the execution of the study and the development of valuable insights into the mathematical modeling of motorcycle tire characteristics.

7. REFERENCES

[1] Nakajima Y., Advanced Tire Mechanics: Volume 2. Springer; 2019.

[2] Horne W.B., Joyner U.T., and Leland T.J.W., Study of the retardation force developed on an aircraft tire rolling in rush or water. Washington, National Aeronautics and Space Administration, 1960. (Technical Note; D-552).

[3] Horne W.B., and Leland T.J.W., Influence of tire tread pattern and runway surface sondition on breaking friction and rolling resistance of a modern aircraft tire. Washington, National Aeronautics and Space Administration, 1962. (Technical Note; D-1376).

[4] Horne W.B., Tire hydroplaning and its effects on tire traction. Highway Research Record, 1968, pp. 24–33.

[5] Gallaway B.M., Schiller R.E., and Rose J.G., The effects of rainfall intensity, pavement cross Slope, surface texture, and drainage length on pavement water depths, Texas Transportation Institute, College Station, 1971.

[6] Gallaway, B.M., Hayes G.G., Ivey D.L., Ledbetter W.B., Olson R.M., Ross H.E.Jr., Schiller R.E.Jr., and Woods D.L., Pavement and geometric design for minimizing hydroplaning potential, Texas Transportation Institute, College Station, 1979.

[7] Huebner R.S., Reed J.R., and Henry J.J., Criteria for predicting hydroplaning potential, J. Transp. Eng., Vol. 112, Issue 5, 1986, pp. 549-553.

[8] Suvanjumrat C., Comparison of turbulence models for flow past NACA0015 airfoil using OpenFOAM, Engineering Journal, Vol. 21, Issue 3, 2017, pp. 207–221.

[9] Chaichanasiri, E. and Suvanjumrat C., Simulation of three dimensional liquid-sloshing models using C++ open source code CFD software, Kasetsart Journal (Natural Science), Vol. 46, Issue 6, 2012, pp. 978–995.

[10] Baranowski P., Malachowski J., and Mazurkiewicz L., Numerical and experimental testing of vehicle tyre under impulse loading conditions, Int. J. Mech. Sci., Vol. 106, 2016, pp. 346-356.

[11] Baranowski P., Janiszewski J., and Malachowski, J., Tire rubber testing procedure over a wide range of strain rates, J. Theor. Appl. Mech., Vol. 55, 2017, pp. 727-739.

[12] Phromjan J. and Suvanjumrat C., Non-pneumatic tire with curved isolated spokes for agricultural machinery in agricultural fields: Empirical and numerical study, Heliyon, Vol. 9, 2023, pp. e18984.

[13] Liu M.W., Oeda Y., and Sumi T., Modeling free-flow speed according to different water depths - from the viewpoint of dynamic hydraulic pressure, Transport Res. D-Tr E., Vol. 47, 2016, pp. 13-21.

[14] Rugsaj R., and Suvanjumrat C., Finite element analysis of hyperelastic material model for non-pneumatic tire, Key Engineering Materials, Vol. 775, 2018, pp. 554-559.

[15] Wong J.Y., Theory of Ground Vehicles, Wiley, 2008.

[16] El-Sayegh, Z., and El-Gindy M., Modelling and prediction of tyre–snow interaction using finite element analysis – smoothed particle hydrodynamics techniques., Proceedings of the Institution of Mechanical Engineers, Part D: Journal of Automobile Engineering, Vol. 233, Issue 7, 2018, pp. 1783-1792.

[17] Phromjan J., and Suvanjumrat C. Material properties of natural rubber solid tires for finite element analysis, Key Engineering Materials, Vol. 775, 2018, pp. 560-564.

[18] Phromjan J., and Suvanjumrat C., Effects of load and velocity on vibrations of a solid tire: experimental study, Songklanakarin J. Sci. Technol., Vol. 43, Issue 1, 2021, pp. 229-236.

[19] Rugsaj R., and Suvanjumrat C., Dynamic finite element analysis of rolling non-pneumatic tire, International Journal of Automotive

Technology, Vol. 22, Issue 4, 2021, pp. 1011-1022.
[20] Phromjan J., and Suvanjumrat C., The contact patch analysis of solid tire on drum testing by finite element method, IOP Conf. Series: Materials Science and Engineering, Vol. 886, 2020, pp. 012049.
[21] Phromjan J., and Suvanjumrat C., The contact patch characterization of various solid tire testing methods by finite element analysis and experiment, International Journal of GEOMATE, Vol.19, Issue 76, 2020, pp. 25-32.
[22] Rugsaj R., and Suvanjumrat C., Development of a novel spoke structure of non-pneumatic tires for skid-steer loaders using finite element analysis, Mech. Based Des. Struct. Mach, Vol.51, Issue 12, 2023, pp. 6905-6927.
[23] Chakrit S., and Rugsaj R., The dynamic finite element model of non-pneumatic tire under comfortable riding evaluation. GEOMATE Journal, Vol. 19, Issue 76, 2020, pp. 62-68.
[24] Rugsaj R., and Suvanjumrat C., Development of a transient dynamic finite clement model for the drum testing of a non-pneumatic tire. IOP Conference Series: Materials Science and Engineering, Vol. 886, 2020, pp. 012056.
[25] Phromjan J., and Suvanjumrat C., Effects on spoke structure of non-pneumatic tires by finite element analysis. International Journal of Automotive Technology, Vol. 23, Issue 5, 2022, pp. 1437-1450.
[26] Rugsaj R., and Suvanjumrat C., Mechanical characteristics of airless tyre by laboratory testing, IOP Conference Series: Materials Science and Engineering, Vol. 773, 2020, pp. 012037.